February 1973 LRP 60/73

A DOUBLE DISCHARGE HIGH POWER TEA CO_2 LASER

P. Boulanger, A. Heym, J.-M. Mayor and Z.A. Pietrzyk

A b s t r a c t

A double discharge TEA CO_2 laser of simple design and easy operation has been successfully operated; the output energy is 12 Joules, the power 0.5 Gigawatt of linearly polarized light. The influence of the different gas mixtures on the problem of arcing, time delay before lasing and evolution in time of the light pulse, has been investigated. The addition of xylene, tried to our knowledge for the first time in a TEA laser, made possible the operation of a long and narrow laser configuration. Xylene avoid the formation of arcs in a very efficient way. This permits in a given geometrical electrodes configuration to increase the input energy in the glow discharge. This way 200 Joules per liter were fed in the glow discharge without arcing. The laser described in this paper is capable of a power output of 42 MW per cm^2 of the beam cross-section. The maximum efficiency is 6.5 %.

Lausanne

Some CO_2 laser requirements in plasma physics

Since the pioneering article of Beaulieu (1), transversely excited atmosphere CO_2 lasers are the most active field in laser research. Their discovery stirred a great interest in plasma physics,as high power lasers are useful for heating and diagnostic purpose.Heating is obtained by passing the laser beam through the plasma. The photon may be absorbed by various processes giving its energy to the ionized gas; this heating method is of high interest with CO_2 laser as they have a high efficiency (2) (4 to 20 %), compared to the previously used Nd or Ruby high power lasers. The best transfer of energy is obtained when the frequency of the laser is equal to the plasma frequency. At 10.6 μ, the corresponding frequency would be equal to the plasma frequency in a plasma of density 10^{19} electrons cm^{-3}. This density is between the density of a solid (10^{22} $e.cm^{-3}$) and the density of magnetically confined high temperature plasma (10^{16} - 10^{17} $e.cm^{-3}$). CO_2 lasers are used for pellet heating at the solid density (3) and heating of pinches (4); around 10^{17} $e.cm^{-3}$ the absorption length is around 10^5 cm at 10.6 μ. Hopefully for very large laser power it is predicted that non linear mechanism of absorption might reduce this length. Recent calculations (5) have shown that CO_2 lasers were now the nearest kind of laser to satisfy to breakeven requirements for fusion generators.

For optical diagnostics, CO_2 laser is mainly used in interferometry and light scattering. In interferometry its large wavelength makes it 15 times more sensitive than He-Ne lasers. For scattering the high value of the ratio λ/λ_D (λ_D Debye length in the plasma) makes the "collective" scattering regime more easily attainable than at smaller wavelength. For both applications the CO_2 laser must satisfy a set of requirements.

- In order to have a good signal to noise ratio for scattering, the power must exceed 100 MW. The power requirement for interferometry is less severe although the higher the power, the easier the measurement.

- To obtain a good time resolution of short lived plasmas (lasting a few μsec) the laser pulse should be of short duration: less than 100 nsec.

- Although it can be monitored the laser output must be reproducible within 20 %.

- The time delay between electrical discharge and light pulse must be controlled accurately (jitter reduced to a low level). The time evolution of the pulse must be reproducible.

- The divergence of the laser should be reduced to the diffraction limit.

- Ideally for light scattering, light should be linearly polarized, which increases the signal over noise ratio by a factor 2 when compared to non polarized light.

Introduction

There has been various electrode configurations used for exciting without arcs the gas mixture in the laser cavity. The earliest and easiest was the resistively loaded pin electrode system (1,6) in which the arc formation is prevented by limiting the current in each pin by a serie resistor. This system has several drawbacks. The

efficiency is substantially lowered by energy dissipation in the resistors and the energy input is also limited; thus loaded pin electrodes lasers are only convenient to excite small volume of gas. For energy larger than one Joule, double discharge CO_2 lasers have been successfully operated (7,8,9): a first pulse (preionization) ionises the gas in the laser cavity. Then the main bank is discharged and for good preionization and fast discharges, the voltage has dropped between the two main electrodes before an arc may develop. The instability mechanisms which lead to arc formation are not well understood; it has been attributed to cathode processes involving field emission, local heating and other space charge distortion of the cathode electric field (10); whatever their cause arc are avoided by good preionization and fast discharge. The double discharge system is of simple conception but not optimized: in order to keep a sufficient rate of ionization, the electric field has to be much higher than the ideal one. It should be so that an electron between two collisions gain an energy corresponding to the maximum excitation cross-section of either CO_2 (001) or N_2 (1-8) vibrational levels. For CO_2 excitation this corresponds to 4 Kv/cm. In electron beam controlled CO_2 laser (11), electrons are created independently of the main discharge in the volume between the two electrodes by an electron beam. Then the optimum voltage may be applied between the two electrodes. This procedure although obviously preferable is much more delicate and costly than double discharge lasers. The system described in this paper is a double discharge CO_2 laser which satisfy the requirements enumerated in the first paragraph. Study of the influence of the gas mixtures indicated that N_2 favours the arcing and our laser could not be operated above a concentration 20 % of N_2. It was proven that in these high field (15 to 20 Kv/cm^{-1}) N_2 was also responsible for population inversion; the amount of energy fed into the laser was 200 Joules l^{-1} for a concentration of 20 % N_2. Primarely

design for high power output per unit surface the coupling to the outside was high (two plane mirrors, one 100 % reflecting another 8 % reflecting), and the efficiency 6,5 %.

Description and use of the apparatus

The double discharge laser consists of three electrodes as shown in Fig. (1). The bottom copper one is shaped in Rogowsky profile. The main discharge is fired between the bottom electrode and the mesh electrode made of a fine grid of stainless steal (mesh spacing = 1 mm). The discharge volume is 4 x 3 x 110 cm.

Above the mesh electrode there are twelve rows of 200 pins each. Where the preionization occurs distance between pins and mesh is 1 cm. The very simple electrical circuit is shown in Fig. (2). A Marx generator consisting of two capacitors (C_1 = 0.1 µF) with two spark gaps, creates a fast rising potential between the mesh and the other two electrodes. Because of the high curvature of the pins points and the small spacing, discharge occurs first between pins and mesh until capacitor C_2 (C_2 = 1000 pF) is charged; this is the preionization circuit. Then the discharge develops in the main gap. The capacitors are charged up to 50 KV. Contrary to a similar circuit (7), all the pins are connected to the same capacitor C_2. Independent feeding of each row of pins to a small capacitor was tried without noticeable improvement. In a first system delay was introduced between preionization and main discharge. No amelioration was observed for delay between 0 and 0.6 µs and it was dropped later, leaving a simpler circuit. To prevent arcing, the energy has to be deposited in a time short compared to the arc formation time: the self-inductance of the circuit is lowered as much as possible by using

wide connections and making the system compact. Its value is 0.5 μH. The electrodes system is attached to a plexiglass gas light housing. The cavity is always operated at atmospheric pressure with a gas flow of 7 $L.min^{-1}$. In parallel with the main gas flow, a by-pass is set up to have part of the gas mixture bulbing through xylene (bi-methyl-benzene C_8H_{10}). The partial pressure of xylene favorable to avoid arcing is about 1 Torr (14). The plexiglass housing was closed on one side by a 100 % mirror and on the other side by a Brewster angle Na Cl window. The second mirror consists of an Na Cl flat plate. The optical resonator length is 1.5 m. No degradation of the apparatus is noticeable except the Na Cl flat mirror which exploded in various spots after few thousands shots.

Characteristics of the laser

Voltage current measurements

The shape and duration of the voltage-current measurements of the discharge depend very slightly on the gas mixture. A typical measurement is shown in Fig. (3).

A total current of 13 KA or 40 A cm^{-2} is flowing through the plasma without arc. When an arc occurs, the resistance drops below the critical resistance $2\sqrt{\frac{L}{C}}$ and the discharge oscillates. The beginning of the arc is noticed by an abrupt slope change, Fig. (4).

Energy

The laser energy is measured by a plexiglass-copper calorimeter (12): the energy of the beam is absorbed in plexiglass; the heat is trans-

ferred to copper which rise of temperature is measured.

Lasing occurs even when an arc cuts the discharge; the energy is then decreased by a factor four. All the results indicated in the rest of the paper are taken in reliable conditions without arcing.

Fig. (5) shows the output energy versus voltage and Fig. (6) the laser efficiency versus voltage. No measurement are possible below 65 KV as the preionization is then too weak to avoid arcing the main gap.

The maximum efficiency occurs for the electric field equal to 17 KV/cm. (The optimum mixture is 20 % N_2, 30 % CO_2, 15 % H_2, 35 % He) . Above 20 % N_2, it is not possible in our laser to prevent arcing. Bigger percentage of CO_2 does not give higher output. A study of the light output of the laser varying the relative proportion of helium and hydrogen shown in Fig. (7) indicates that hydrogen at high concentration reduces the laser efficiency. This was observed too in (11). However, small percentage at hydrogen does not change energy output very much: for 10 % of H_2 energy is lowered only by 5 %.

It was observed that the value of the electrical current was dependent on the gas mixture used in the discharge. It was important to determine whether the increase of light energy output observed for the different proportion of He/H_2 was due either to an increase in energy input

$$\varepsilon(t) = \int_0^t v(\tau)\, I(\tau)\, d\tau$$

at the time of the laser pulse (t_1 = 350 ns for 20 % of N_2 concentration), or to a stronger depopulating effect of He on the 020 CO_2 level.

To decide between those two possibilities the value of $\varepsilon(t)$ was measured, Fig. (8), for different gas mixture. The total energies $\varepsilon(t = \infty)$ were normalized to 1 in order to avoid errors due to the calibration coefficients (also the total energy was only changed by 3 %). The variation $\varepsilon(t_1)$ was only 9 % for concentration of H_2 between 5 and 30 % while the light output energy variation was 25 %. Although the first alternative cannot be completely dismissed as unimportant, the second effect - the depopulating effect of He through vibrational-translational energy exchange - seems predominant.

For the future of the laser, it is useful to know if it is possible, for a given geometrical configuration and a gas mixture, to increase the energy input per unit volume. To check this possibility part of the laser discharge was covered by a plastic sheet, the discharge was limited in a part of laser volume. By covering bigger part of the discharge, it was possible to reach the point when it was not possible to have a discharge without arcs.

Only ~ 12 % of discharge length could be covered without arcing. This seems to indicate that only 12 % more energy could be fed in the discharge for our electrodes configuration and gas mixture (20 % N_2 , 30 % CO_2, 15 % H_2, 35 % He).

When the laser was shorten by ½ at its length, the strong arc occurs between electrodes. The current in the circuit was measured for this case. From decreasing amplitudes of oscillating current the resistance and inductance at the external circuit were calculated. The resistance calculated that way is mainly resistance of the external circuit and its value is about 0.15 Ω.

From the voltage - and current time dependence - the resistance of the discharge plasma was also calculated, Fig. (9). Lowest resistance

(without arcs between electrodes) is around 5-6 Ω. Comparison of this resistance with the external resistance shows a very high (> 98 %) electrical efficiency of the system.

The influence of xylene on energy output was also investigated. A minimum and maximum amount of xylene, necessary to avoid arcing, was measured. In most cases, the maximum concentration was about twice the minimum value. Between this two borders no change of energy output was observed. The typical value for amount of xylene is $8 \cdot 10^{-2}$ %.

Power

The shape of the pulse is measured by a photon drag detector. Typical result is shown in Fig. (10). A sharp light pulse is sometimes followed by a long tail, Fig. (11), of small amplitude or even a smaller second pulse Fig. (12). The pulse shape, the delay between the instant the voltage is applied on the electrodes and the laser pulse, and the power emitted depend on alignment, gas mixture and Q value of the cavity.

a) Delay

The time elapsed between spark gap firing and laser pulse is remarkably reproducible when all parameters are kept constant Fig. (13). This delay is slightly dependent on alignment: when the laser is misaligned, losses are bigger and the time necessary for "gain switching" is longer. The same phenomena is observed when a diaphragm is introduced in the cavity: the diffraction losses increase the gain switching delay. The delay depends on the concentration of N_2. At high electric field the excitation cross-section for N_2 is larger than CO_2 (13) and almost all CO_2 is pumped indirectly through N_2 excited molecules. Henceforth, when the proportion of N_2 decreases, the delay increases. With a Na Cl flat

mirror, lasing does not occur for less than 5 % N_2. The delay of laser action after the beginning of current versus concentration of N_2 is given in Fig. (14).

For 5 % N_2, the lasing occurs after the end of the current pulse. This indicates that CO_2 molecules are excited in the upper vibrationnal level, not by direct electronic impact, but through the Fermi resonance with the first level of N_2. Longer delays for lower apply voltages show slower excitation. At 80 KV the lasing coincides with the end of the current.

With a Germanium output mirror (60 % reflection), instead of a Na Cl flat the higher Q value of the cavity greatly reduces the delay. Concurrently a high energy tail is observed, Fig. (15).

b) Pulse shape

With the optimized mixture (15 % H_2, 35 % He, 30 % CO_2, 20 % N_2) the giant pulse has around 25 ns width at middle height. The power is around 0.5 GW. With 20 % N_2, the light pulse occurs before the end of the current Fig. (10) which is an unfavorable situation as the rest of the current does not create a sufficient population inversion for further laser action. It would be favorable to delay the light pulse until the end of the current either by passive or by active Q switching. Such a switch would increase the output about 30 % (see Fig. (8)). The appearance of tail is eased by misalignment and high N_2 concentration.

The homogeneity of the laser beam was measured with a photon drag detector Fig. (16). The laser beam was focussed on the photon drag detector; in front of the detector, the polyetylene diffusor B was placed. The 5 mm ring diaphragm A was placed in front of the laser. Masking different parts

of the beam permitted the measurements of the spatial dependence of the energy density output.

The lasing is homogeneous and constant over 80 % of the surface. Near the edges of the beam diffraction effects are important and could be annoying for interferometry. Near the cathode small streamers develop during the discharge. They weaken the lasing where they occur.

Divergence

The beam divergence is low. The divergence is diffraction limited to $\theta \sim \frac{\lambda}{a}$, where a is the beam radius. $\underline{\theta} = 10^{-3}$ rad.

Polarisation

The polarisation is measured by reflecting the beam at Brewster angles on a sodium flat. The calorimeter was rigidly fixed to the sodium flat Fig. (17). When the Brewster angle correspond to one polarisation,the energy reflected is hardly measurable (with a calorimeter signal over noise ratio around 1.5). Turning the sodium reflector by 90^{o} around the light beam gives an energy reflected 10 times stronger. The beam is at least 90 % polarised.

Conclusion

The laser described in this paper is very reliable and easy to operate. Its high power output makes it for various plasma diagnostics like scattering and interferometry. The favorable role of xylene in the discharge to avoid arcing has been demonstrated clearly. Some clarifi-

cations are needed about the way preionization really works so that it could be improved and higher energy could be absorbed in the same discharge volume. The electrons may come from photo-ionization due to U.-V. radiation created by corona or arc discharge in the preionization, or by avalanche processes in the main gap.

Acknowledgements

The authors would like to thank Mr. Ripper and G. Ziegenhagen for the precious help they gave in the construction of various part of the apparatus, and Dr. F.S. Troyon for encouraging and stimulating discussion.

References

(1) A.J. Beaulieu, Appl. Phys. Letters 16, 12, 504 (1970)

(2) J.M. Dawson, R.E. Kidder and A. Hertzberg, Matterhorn report 782, Princeton University (1972)

(3) J.L. Bobin, F. Floux and G. Tonon. Quatrième Conférence sur la Fusion Contrôlée, Madison, Wisc. (1971)

(4) N.A. Amherd and G.C. Vlases. Quatrième Conférence sur la Fusion Contrôlée, CO_2 laser heating of a small θ-pinch, Madison, Wisc. (1971)

(5) J.L. Bobin. Laser created Plasmas and controlled thermonuclear Fusion. Fifth European Conference on Controlled Fusion (1972) Grenoble

(6) R. Fortin, Can. J. Phys. 49, 257 (1971)

(7) M.C. Richardson, A.J. Alcock, K. Leopold and P. Burtyn. Proceedings of the Symposium on High Power Molecular Lasers. Quebec (May, 1972)

(8) R. Dumanchin, IInd Conf. Laser Eng. and Applications, Washington DC, U.S.A., May 1971

(9) A.K. Laflamme, Rev. Sci. Instr. 41, 1578 (1970)

(10) C.A. Fenstermacher and al., Appl. Phys. Lett. 20, 2 (1972)

(11) T.F. Stratton and al., Proc. of the Symposium on High Power Molecular Lasers, Quebec (May, 1972)

(12) P. Boulanger, A. Heym, J.-M. Mayor and Z. Pietrzyk. "An absolute calorimeter for high power CO_2 lasers", Submitted to Rev. of Sci. Instr.

(13) W.L. Nigham and J.H. Bennet. Appl. Phys. Letters 14, 8 (1969)

(14) R.L. Schriever. Appl. Phys. Letters 20, 9, 354 (1972)

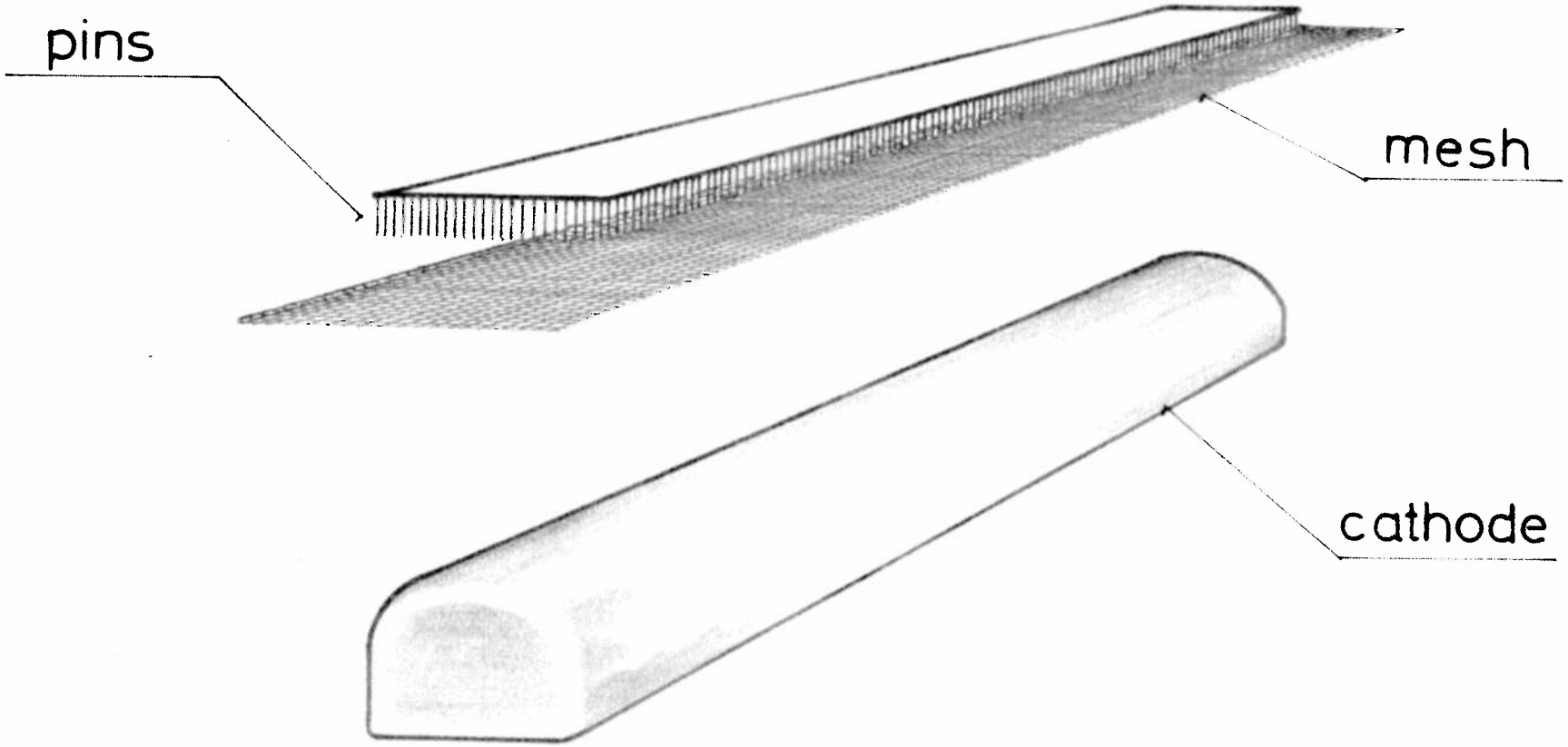

Fig.1 The three electrodes TEA Laser

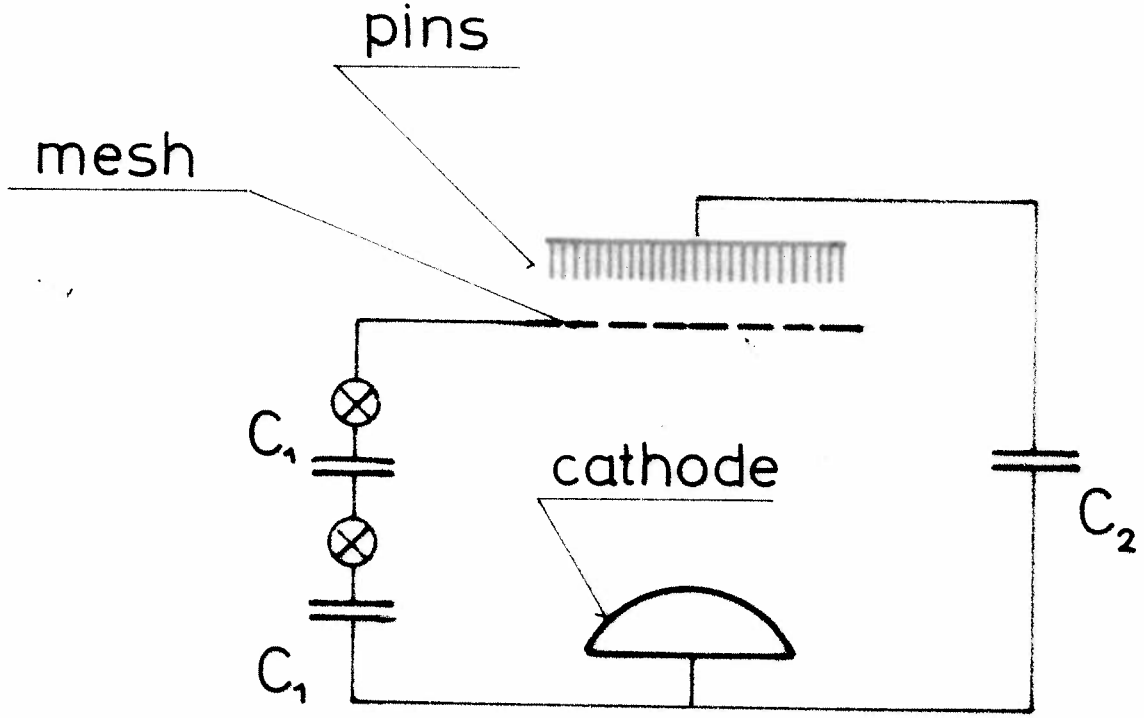

Fig.2 Electrical circuit of the Laser

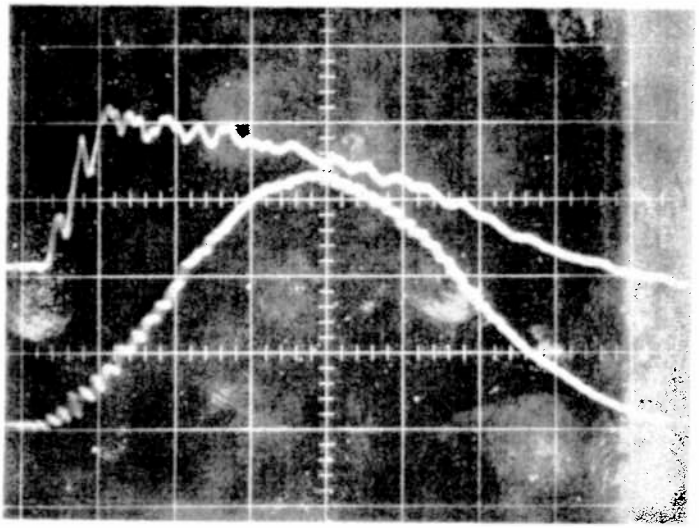

Fig. 3 Voltage current measurement
Upper trace : voltage 50 kV/cm
Lower trace : current 4 kA/cm
Time sweep : 100 ns/cm

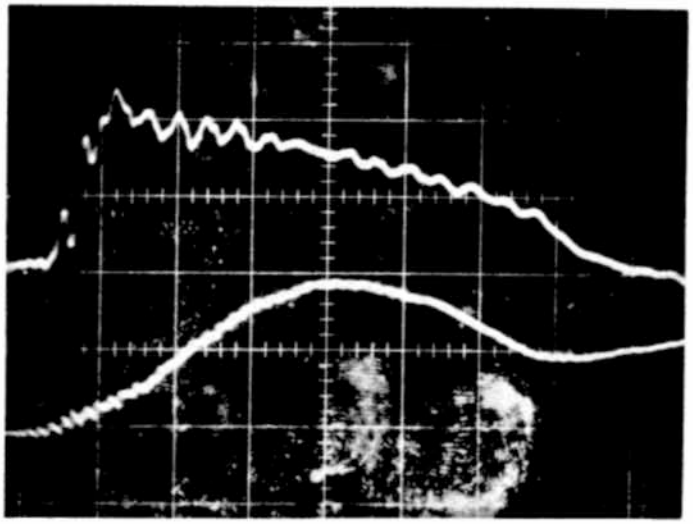

Fig. 4 Voltage current measurement in case of arcing in the laser

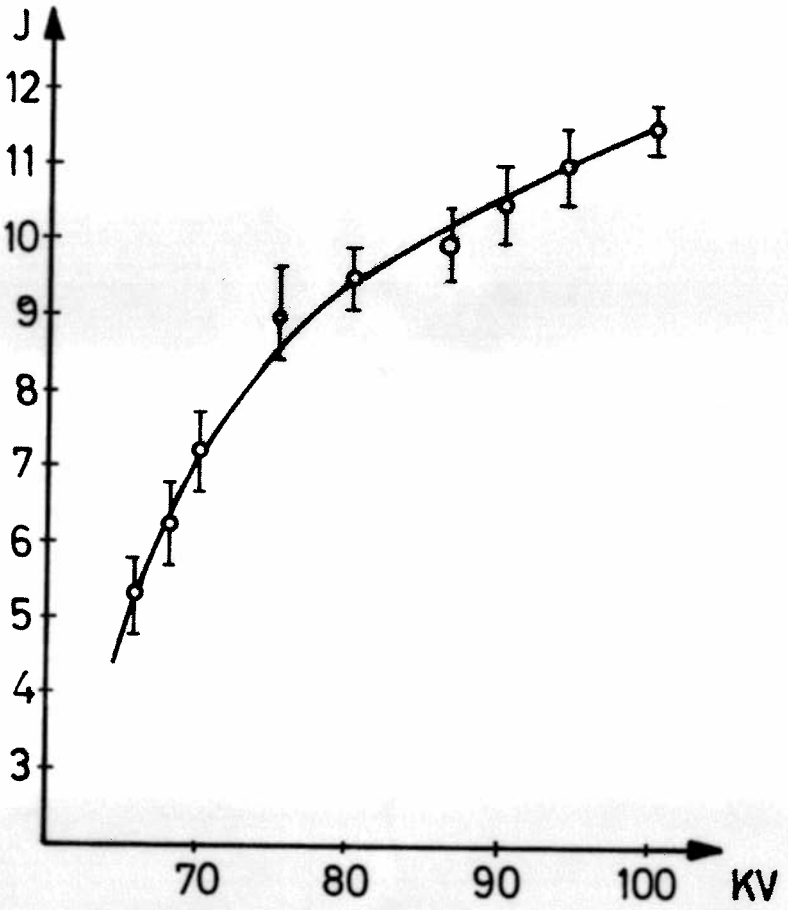

Fig. 5 Output energy versus voltage

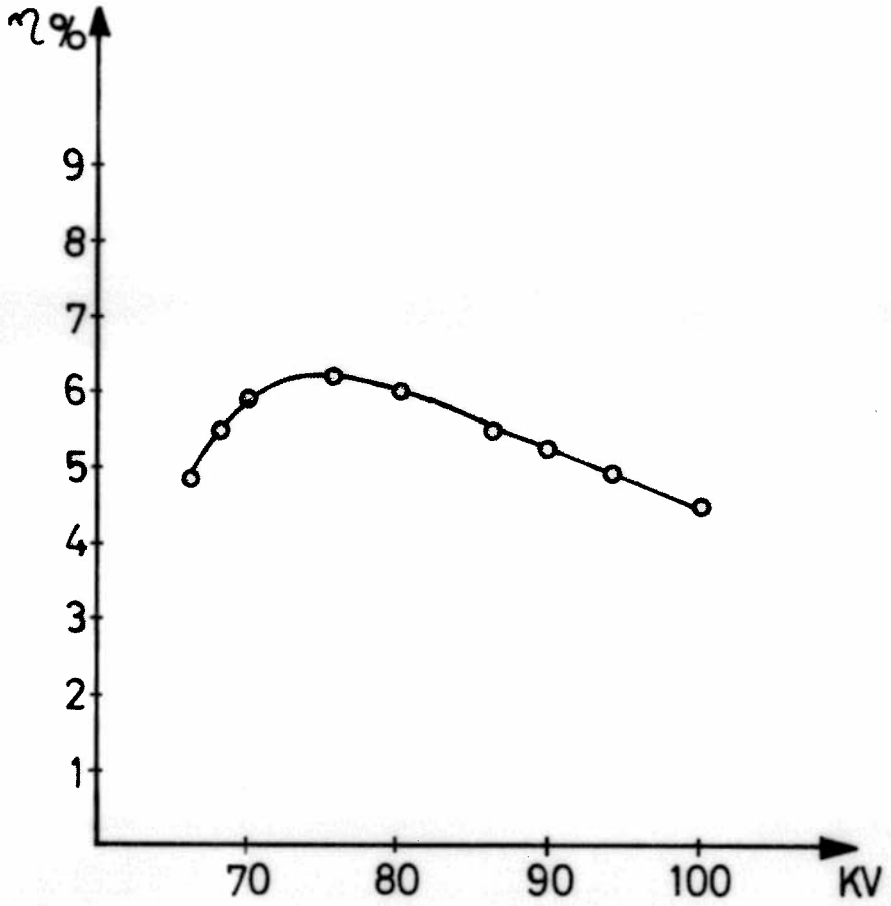

Fig. 6 Laser efficiency versus voltage

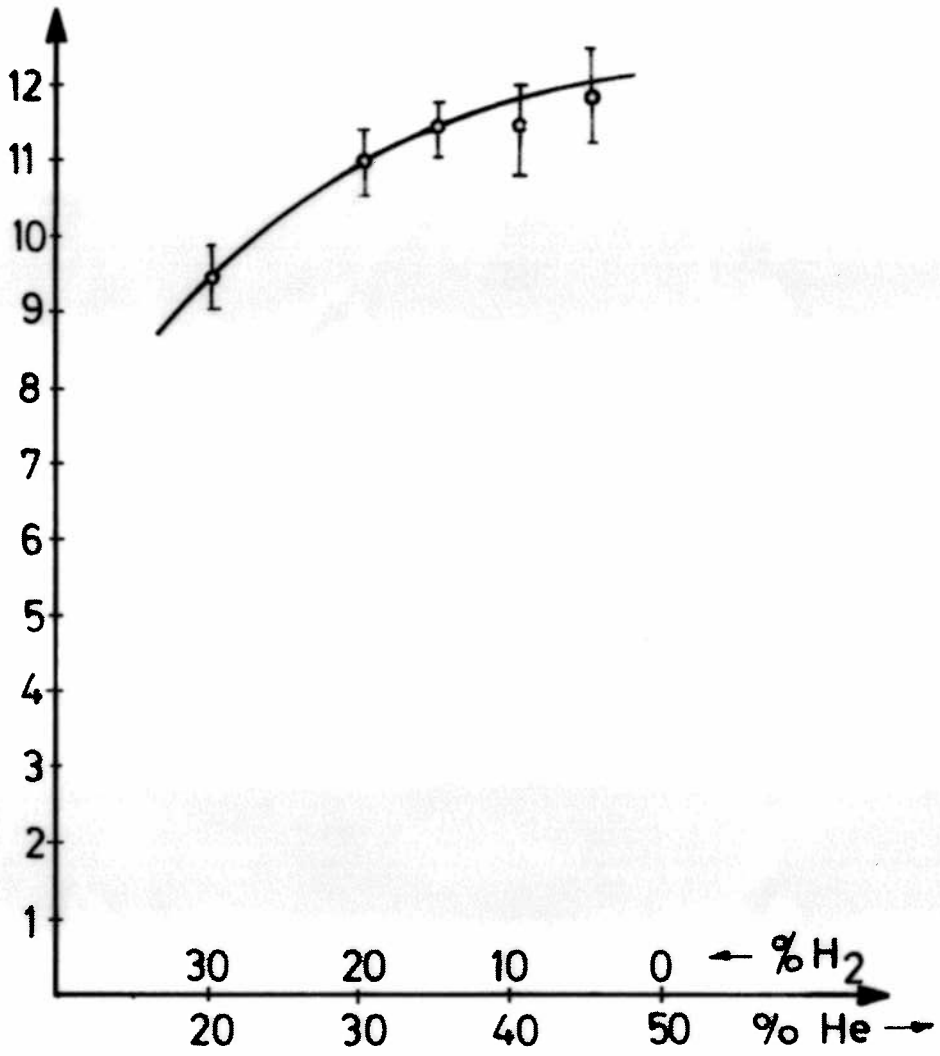

Fig. 7 Energy with relative concentrations of H_2 and He

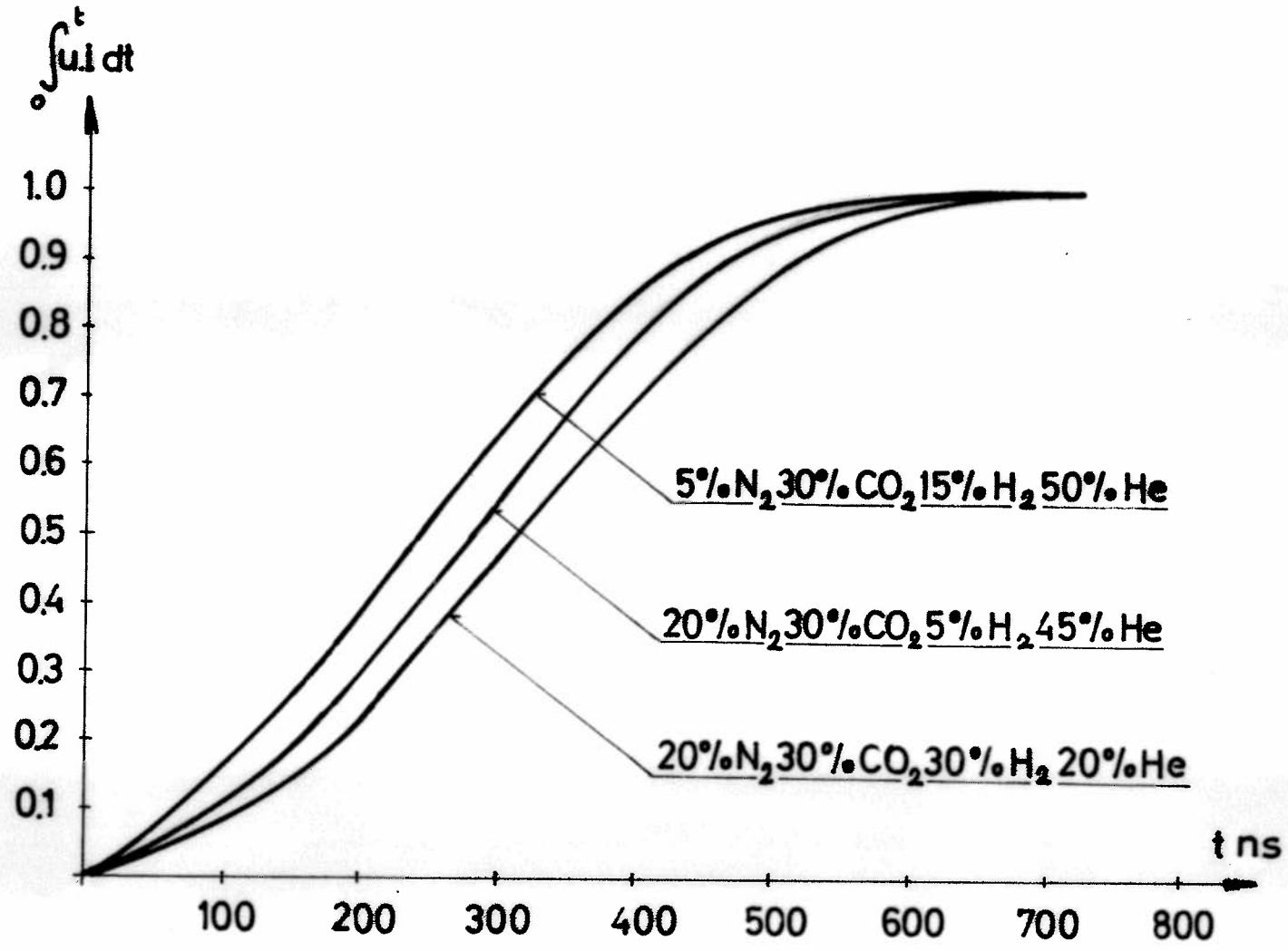

Fig.8 Energy in the discharge versus time.

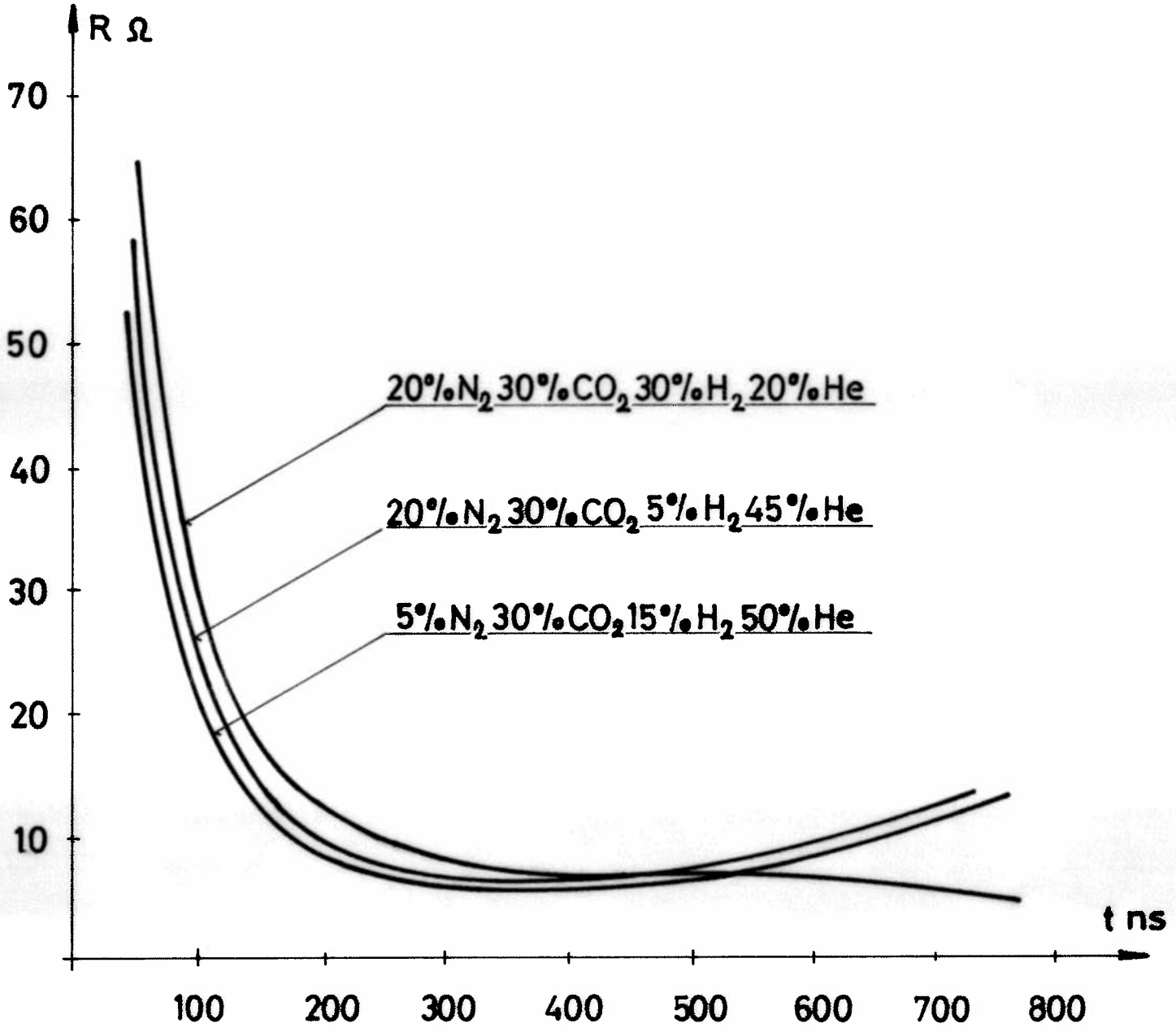

Fig.9 Resistance of discharge versus time.

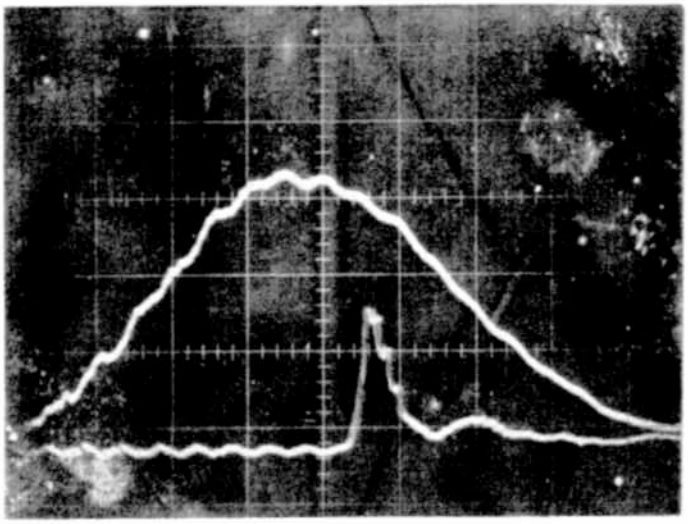

Fig. 10 Current and photon drag measurement.
Time sweep 100 ns/cm

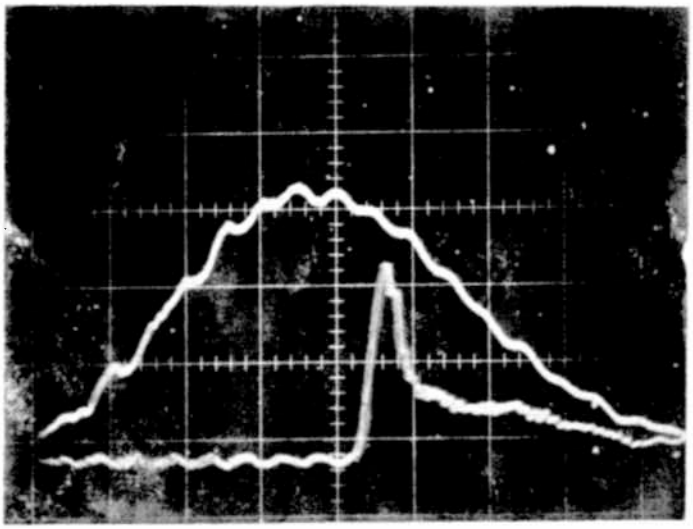

Fig. 11 Current and photon drag measurement.
Pulse with tail

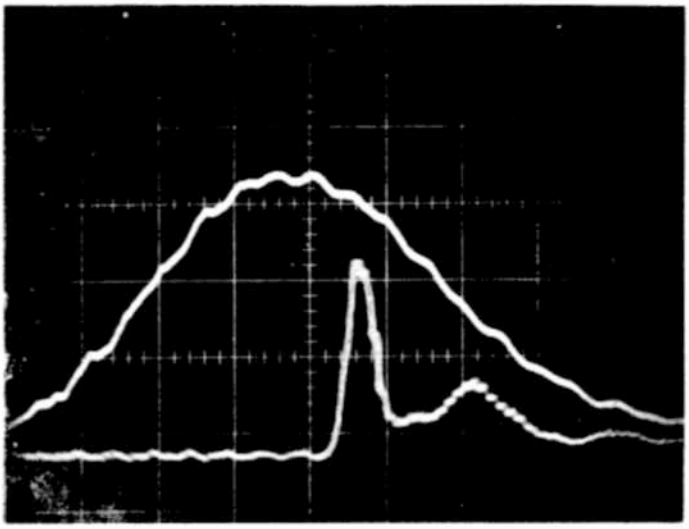

Fig. 12 Current and photon drag measurement. Pulse with the second smaller pulse

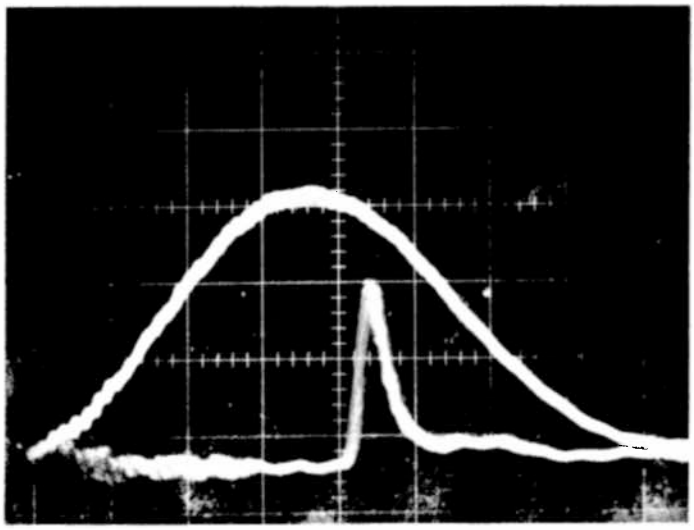

Fig. 13 Current and photon drag measurement. 6 traces on one picture

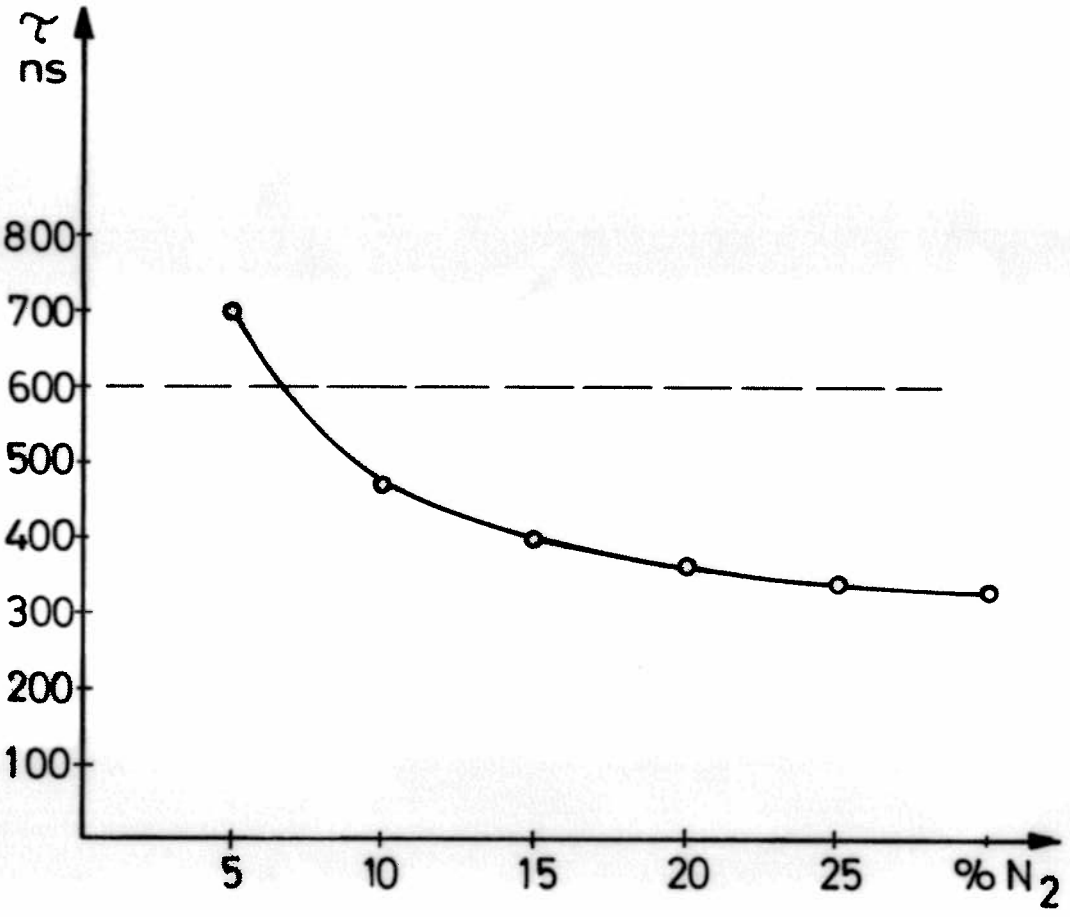

Fig. 14 Delay time versus concentration of N_2

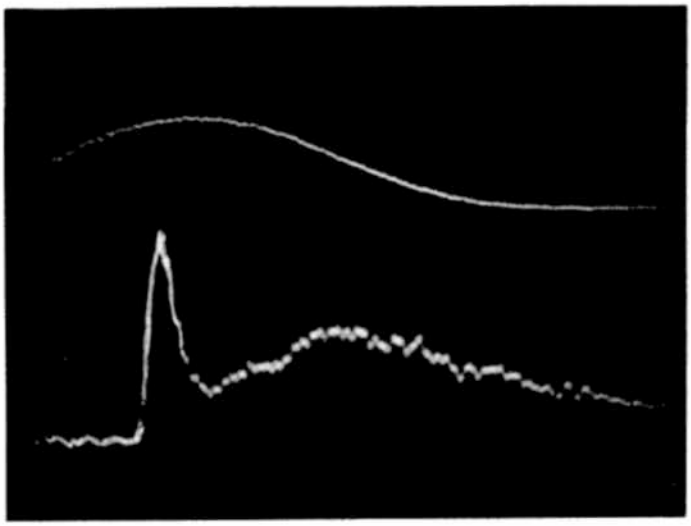

Fig. 15 Current and photon drag measurement, with a Germanium output mirror

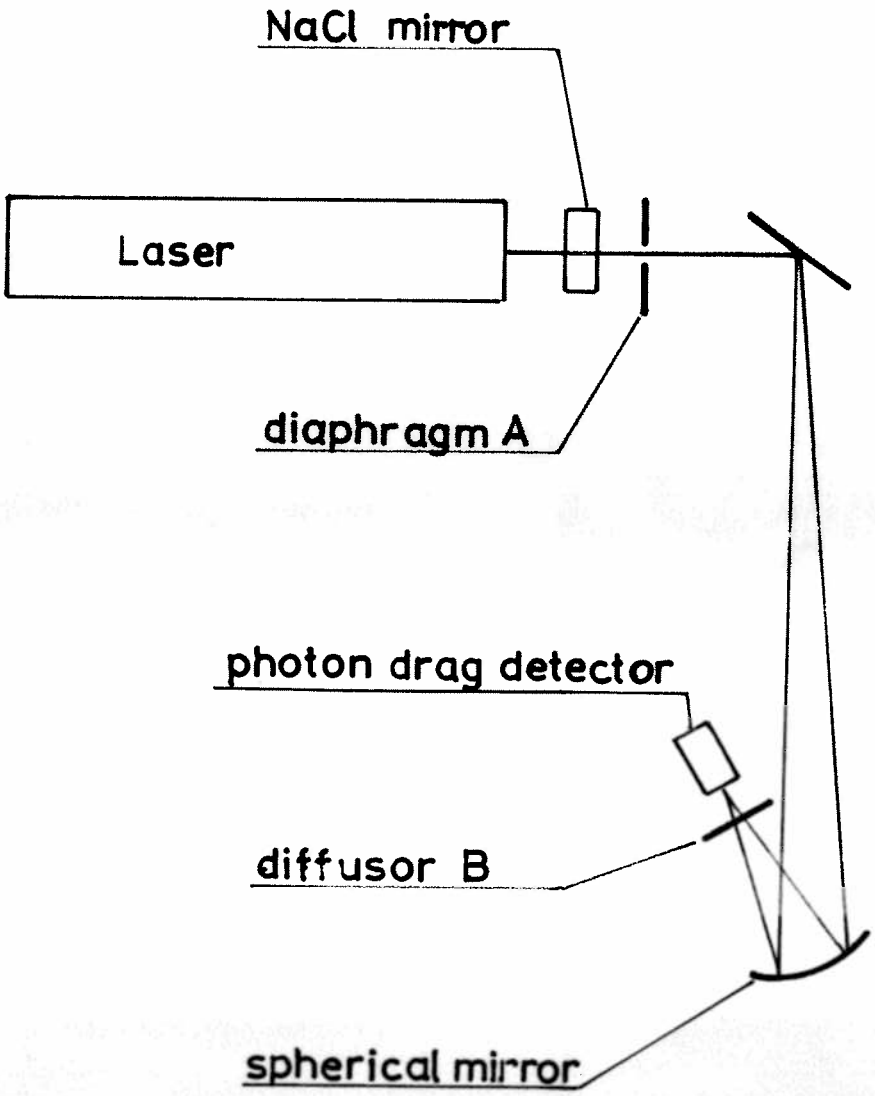

Fig. 16 The measurement of beam homogenity.

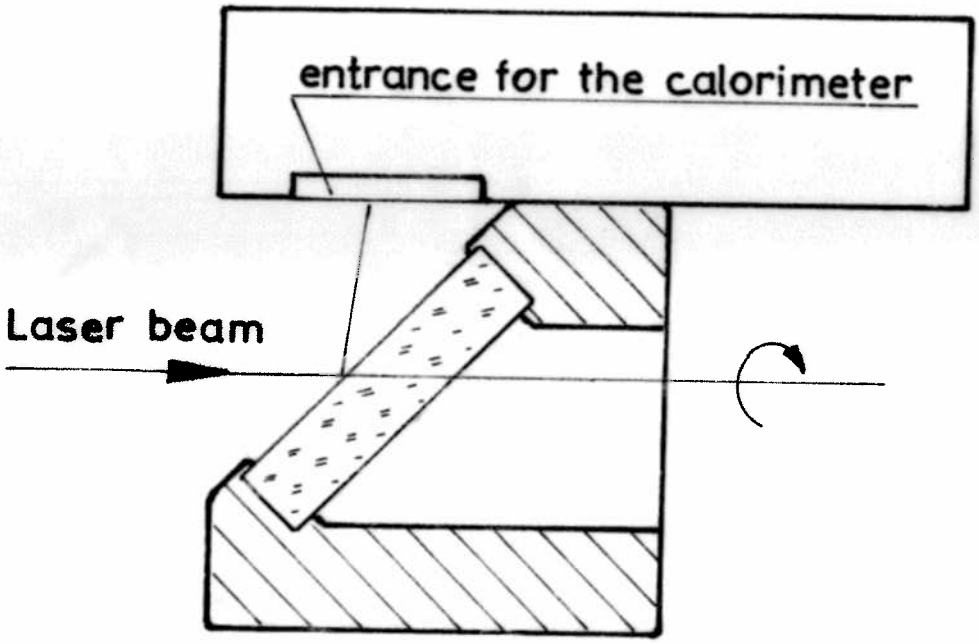

Fig.17 The measurement of Laser beam polarization.